THE EFFECT OF THE MELT TEMPERATURE AND THE COOLING RATE ON THE MICROSTRUCTURE OF THE Al-20% Si ALLOY USED FOR MONOLITHIC ENGINE BLOCKS

W. Kasprzak and M. Sahoo
CANMET Materials Technology Laboratory, Ottawa, Ontario, Canada

J. Sokolowski
University of Windsor, Windsor, Ontario, Canada

H. Yamagata and H. Kurita
Yamaha Motor Co. Ltd., Iwata, Shizuoka, Japan

Abstract

The Al-20%Si melt heated to 785°C (1445°F) and 850°C (1562°F) exhibited refinement of the primary Si while heating to 735°C (1355°F) produced coarse and heterogeneous primary Si crystals following the solidification process at approximately 1.3, 4.5, 15 and 35°C/s. The primary Si crystals were 40% finer for the samples heated to 850°C (1562°F) as compared with those heated to 735°C (1355°F). Higher cooling rates produced better primary Si refinement and minimized its variation caused by the melt temperature. The secondary dendrite arm spacing (SDAS) was not affected by the melt temperature and was a function of the cooling rate for the given experimental conditions. The SDAS changed from approximately 32 to 22µm for a 1.3 and 4.5°C/s cooling rate and was reduced to approximately 11µm for a 35°C/s cooling rate. Cooling curve analysis was used to analyze the sequence of the metallurgical transformations and fraction liquid development during alloy melting and solidification. The non-equilibrium thermal characteristics under cooling rate up to 15°C/s were analyzed as well. The experimental results were used to optimize the casting process and improve the service characteristics of the vacuum assisted high pressure die casting (HPDC) motorcycle engine blocks.

Keywords: *Al-Si hypereutectic alloy, high pressure die casting, melt temperature, cooling rate, primary Si, secondary dendrite arm spacing, non-equilibrium thermal analysis*

Introduction

Hypereutectic Al-Si alloys proved to be an excellent choice of materials for high performance automotive cast component applications. A combination of satisfactory wear resistance, cooling characteristics and weight reduction makes these materials a good candidate for monolithic engine block applications.[1-7] Increased concentration of Si minimized the thermal expansion coefficient and improved the alloy's thermal conductivity by almost 3 times in comparison with cast iron.[8,9] Use of monolithic hypereutectic Al-Si engine blocks increased the horsepower and displacement as compared to the cast iron blocks and aluminum blocks with cast iron liners.[2] The tribological properties were mainly controlled by the primary Si size and its distribution as well as its exposure height from the aluminum matrix. Primary Si crystal characteristics cannot be changed by post casting processing (i.e. heat treatment), hence optimum melt treatment and solidification process conditions are critical in obtaining the required tribological properties.[10-15] It was reported that the primary Si particles diameter in the range between 380 and 80µm resulted in satisfactory wear resistance (negligible scoring of the cylinder walls).[2] Adequate refinement of the primary Si crystals is of key importance and creates a technological challenge particularly for slowly solidified cast components or their particular sections. Despite the recent advancements in light metals casting technologies, control of primary Si crystal size and distribution as well as control of the excessive alloy latent heat still presents a considerable challenge to the metal casting community. The metallurgical principles behind as-cast microstructure development have been investigated for decades. Currently the focus is on refinement of the primary Si crystals achieved by controlled alloying, addition of master alloys and rapid solidification.[1,4,16-22] The scientific thrust is also centered on the mechanical, electromagnetic and ultrasonic melt treatment techniques used to modify the primary Si crystals as well as other structural constituents.[23-26] Powder metallurgy offered an alternative method to achieve satisfactory refinement of the primary Si crystals however, due to the prohibitive cost is used only for selected applications.

Modern light metals casting technologies are very complex and involve a diverse set of variables that must be quantitatively evaluated for process optimization and consequently a high quality product. Progress in the development of thermal data acquisition systems allows researchers to collect more reliable information on individual operations in both laboratory and industrial settings. However, in most cases critical thermal data lacks spatial resolution (especially for higher solidification rates) and cannot be easily collected between various operations.

Recent research carried out by authors[6, 7] quantified the effect of solidification rates on the refinement of the primary Si and modification of the Al-Si eutectic with respect to the HPDC processing. The solidification rates corresponding to the critical section of the castings were estimated based on the comparative thermal and structural analysis and were between 50-85°C/s.

The goal of this publication is to quantify the effect of the Al-20%Si melt temperature and solidification rates on the primary Si size, SDAS and the temperatures of the non-equilibrium metallurgical reactions.

Experimental Procedures

Alloy Chemistry and the Test Sample Design

The Al-20%Si alloy chemical composition listed in Table 1 was used in the following studies. This phosphorus modified alloy was specifically developed for the vacuum assisted HPDC technology used for motorcycle monolithic engines blocks.[6,7,15,27]

The first series of experiments were performed using cylindrical test samples with a diameter of φ = 16mm and a length of l = 18mm. These samples were extracted from a production ingot. Each sample had a predrilled hole in the center to accommodate a thermocouple that collected the thermal data and controlled the processing parameters (i.e. temperature, time, heating and cooling rates). The size of the macro test sample was sufficient for the subsequent metallurgical analysis as well as mechanical testing.

Thermal Analysis During Alloy Melting and Solidification Cycles

Thermal analysis during the melting and solidification cycles was carried out using the UMSA Platform.[30] The test samples were processed in low thermal mass crucibles manufactured from a low density ceramic (~0.28g/cm^3) and steel foil used for a circumferential surface. The ratio between the test sample mass (16g) and the mass of its container was approximately 10:1. This design considerably reduced the thermal inertia and improved the thermal signal to the noise ratio. In order to assure high repeatability and reproducibility of the thermal and metallographic data from the melting and solidification experiments, the test sample mass was 16±0.2g. The melting and solidification experiments were carried out in an ambient air environment. The procedure comprised of the following steps: First, the test samples were heated to the predefined temperature and isothermally kept within the range of ±0.2°C for a period of 25 minutes in order to stabilize the melt conditions. The melting rate was kept constant. Next, the test samples were solidified using approximately 1.3, 4.5 and 15°C/s average cooling rates, that were representative of the sand casting (<5°C/s) and low pressure permanent mold (LPPM) technologies (>10°C/s).

In order to assure rapid temperature response, very low thermal mass thermocouples were utilized. The thermal analysis signal in the form of heating and cooling curves was recorded during the melting and solidification cycles. The temperature vs. time and the first derivative vs. temperature curves as well as the fraction liquid / solid vs. temperature curves were calculated and plotted. The melting rate was calculated between the non-equilibrium solidus (start of the melting process) and the non-equilibrium liquidus (end of the melting process) temperatures, i.e., 504.1°C (939.4°F) and 701.9°C (1295.4°F) and was equal to approximately 0.75°C/s. The conventional average cooling rate is calculated between the non-equilibrium liquidus and solidus temperatures.[14,28,29] The authors chose to calculate the cooling rate between 730°C (1346°F) and 380°C (716°F) that corresponded to the melt injection into the die and the removal of the casting respectively in the industrial HPDC process.

The fraction liquid curve obtained during the melting cycle was determined by calculating the cumulative surface area between the first derivative of the heating curve and the base line. The base line represented the hypothetical first derivative of the melting curve that did not exhibit metallurgical transformations during the melting process. The area between the two derivative curves (calculated between the solidus and liquidus temperatures) was proportional to the latent heat of melting of the given alloy. Therefore, the latent heat of the melting process affected the fraction liquid evolution.

Solidification Experiments Under Slow Cooling Rates

Cylindrical test samples were heated to 735°C (1355°F), 785°C (1445°F) and 850°C (1562°F), then held for 25 minutes and solidified under natural heat exchange conditions equivalent to a 1.3°C/s cooling rate. An identical experiment was repeated except that the cooling rate was increased to 4.5°C/s using compressed air applied to the outer surface of the test sample. The temperature vs. time signal was collected for subsequent assessment of the thermal characteristics of the solidification cycle. This detailed thermal analysis procedure was described in previous publications.[6,7,14,28,29] This approach allowed for linking of the alloy's thermal and microstructural characteristics.

Table 1. Average Chemical Composition of the Hypereutectic Al-20%Si Alloy (wt%)

Si	Cu	Mg	Zn	Fe	Mn	Ni	Ti	P
20.0	3.0	0.5	0.1	0.5	0.1	0.1	0.001	0.0085-0.011

Note: The targeted P concentration was 0.01%.

Rapid Solidification Experiments in a Copper Mold

A copper mold weighing 12 kg with dimensions of 150x150x76mm (width x length x height) was used to investigate the effect of the melt temperature on the test sample microstructure that solidified under a high cooling rate. The cast cylindrical blocks had an OD = 91mm, a height of 43mm and a mass of 448±15.6g. After preliminary experiments the initial mold temperature was set at 30°C (86°F). A high cooling rate was accomplished by circulating water through the cooling channels inside the mold. The water temperature was controlled by a CARON thermostatic bath with ±2°C accuracy. Based on regression equations obtained from previous studies it was determined that an average cooling rate of approximately 35°C/s could be achieved in the copper mold.[6] This cooling rate is representative of the LPPM technology (>10°C/s) but is lower in comparison with the HPDC (~100°C/s) except these observed in the casting's thick sections. In order to determine the effect of the melt temperature on the as-cast microstructure the alloy was heated in an electric resistance furnace under a protective Argon atmosphere to 735°C (1355°F) and 850°C (1562°F) and maintained for 25 minutes for homogenization. A 2kg siphon ceramic crucible was used for melt transfer and casting of the test samples.

In addition, in order to quantify the effect of the melt pouring temperature on the as-cast microstructure the melt was heated to 850°C (1562°F), homogenized and slowly cooled in a ceramic crucible prior to pouring into a copper mold at 730°C (1346°F). The pouring operation was performed at approximately 45°C (113°F) above the non-equilibrium liquidus temperature. After completion of the casting experiments the test samples were sectioned and prepared for metallographic observations.

Metallographic Assessment of the Test Samples' Microstructure

Perpendicularly sectioned thermal analysis and copper mold test samples were prepared for metallographic analysis using standard procedures. Metallographic analysis for copper mold test samples was conducted 5mm from the bottom of the mold.

An automated Leica light optical microscope linked with the image analysis system was used for determination of the equivalent diameter (ED) of the primary Si particles. The ED was defined as the diameter of the circle having the same area as the analyzed feature. Twenty five (25) analytical fields were analyzed and the average value of the ED and the corresponding standard deviation were calculated. SDAS was measured using the intercept method. Thirty dendrites (30) were analyzed and the average values of the SDAS with the corresponding standard deviation were calculated.

Results

Solidification Experiments Under Slow Cooling Rates

The metallographic analysis of the Al-20%Si phosphorus modified ingots used in this study revealed that the microstructure consisted of coarse primary Si crystals and unmodified Al-Si eutectic as well as Cu based intermetallic phases dispersed in the aluminum matrix.[6,7,15,27] The average ED of the Al-20%Si ingot's primary Si particles was approximately 45µm for targeted 100ppm addition of phosphorus. Thermal analysis of the ingot's heating cycle revealed that the non-equilibrium melting process started at a temperature of 504.1°C (939.4°F) and ended at 701.9°C (1295.4°F) (Figure 1).[6,7] Above this temperature the melt was in a liquid state. The fraction liquid curve obtained during the alloy melting process at a rate of 0.75°C/s indicated that above 585°C (1085°F), (i.e. end of dissolution of Al-Si eutectic) the melt consisted of approximately 83% a liquid phase that contained undissolved primary Si crystals (Figure 1 and Table 2a). A further increase in melt temperature above 585°C (1085°F) resulted in a gradual decrease of the solid phase while the 100% liquid phase was reached at a temperature of 701.9°C (1295.4°F). Exceeding this temperature increased the melt's superheat.

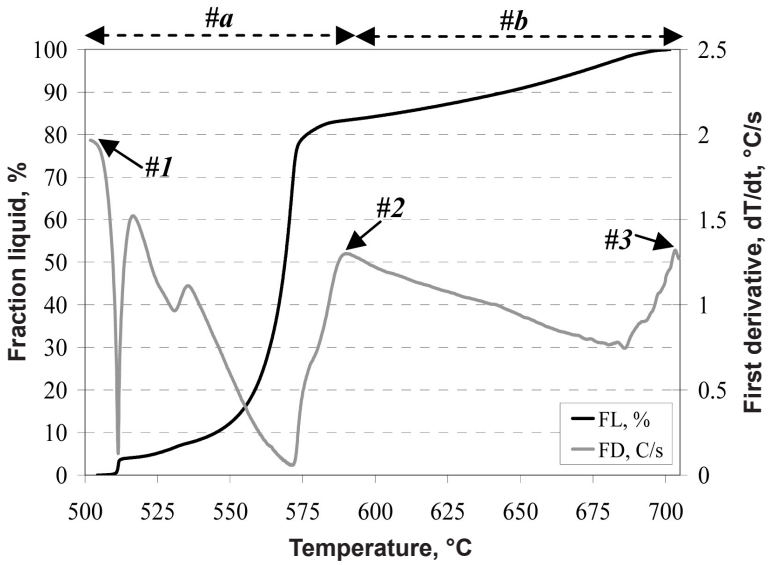

Figure 1. Fraction liquid (FL) and first derivative (FD) vs. temperature curves recorded for the Al-20%Si phosphorus modified alloy during the heating cycle to 785°C (1445F) with an approximate average heating rate of 0.75°C/s. The numbered arrows correspond to the metallurgical reaction and are outlined in Table 2a. The melting range of the Cu based phases and the Al-Si eutectic is indicated by #a while the melting of the primary Si is indicated by #b.

Table 2a. Non-Equilibrium Thermal Characteristics of the Al-20%Si Phosphorus Modified Alloy Obtained During the Melting Process

Points	Thermal characteristics	Average heating rate, 0.75°C/s	
		Temperature, °C (F) / STDEV	Fraction liquid, %
#1	Start of the alloy melting process	504.1±2 (939.4)	0
#2	End of the Al-Si eutectic melting	585.2±5.3 (1085.4)	82.9
#3	End of the alloy melting process	701.9±1.3 (1295.4)	100

Table 2b. Non-Equilibrium Thermal Characteristics of the Al-20%Si Phosphorus Modified Alloy Obtained During the Solidification Process

Points	Thermal characteristics	Average cooling rate, °C/s Temperature, °C (F)/ STDEV		
		1.3	4.5	15
#4	Nucleation of the primary Si (Liquidus temperature)	685.5±1.3 (1265)	700.9±1.3 (1293.6)	713.1 (1315.6)
#5	Nucleation of the Al-Si eutectic	566.0±0.8 (1050.8)	584.8±3.8 (1084.6)	597.1 (1106.8)
#6	Nucleation of the Cu based phases	512.9±1.7 (955.2)	515.4±3.2 (959.7)	512.7 (954.9)
#7	End of solidification (Solidus temperature)	477.2±2.2 (891)	476.3±4.5 (888.8)	482.1 (899.8)
Solidification range		208.3 (406.9)	224.6 (436.3)	231 (447.8)

Temperature vs. time cooling curves recorded for the test samples heated to 735°C (1355°F), 785°C (1445°F) and 850°C (1562°F) are presented in Figure 2a. The average cooling rate calculated between 730°C (1346°F) and 380°C (716°F) was approximately 1.3°C/s and the maximum instantaneous cooling rate was approximately 4°C/s as measured at the liquidus temperature point (Figure 2b). Three visible temperature arrests were noted on the cooling curves (Figure 2a). More detailed information pertaining to the alloy's thermal characteristics such as non-equilibrium liquidus, nucleation of the Al-Si eutectic, etc. was collected from the first derivative vs. temperature curves. The representative curve recorded for the test sample heated to 785°C (1445°F) and solidified at a cooling rate of 1.3°C/s is presented in Figure 2b. The metallurgical reactions are pointed out by the numbered arrows and their corresponding numerical values are presented in Table 2b.

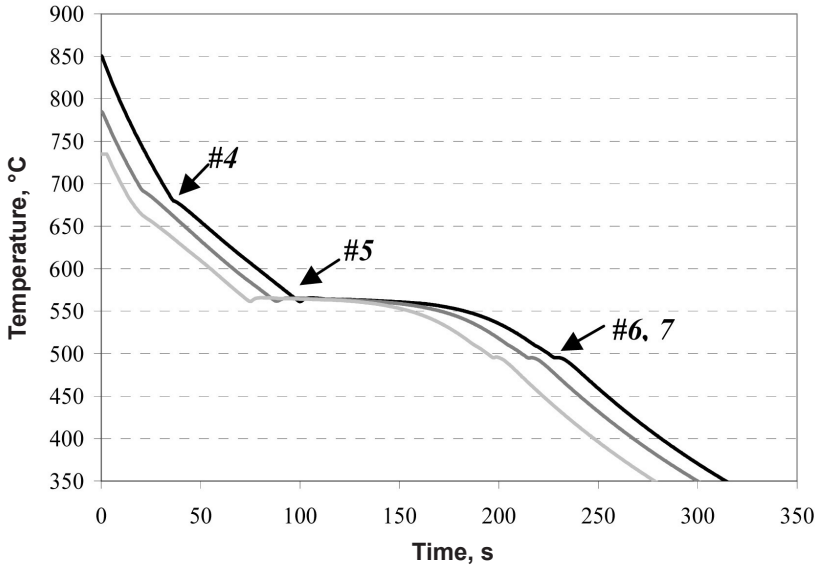

Figure 2a. Temperature vs. time cooling curves recorded for the Al-20%Si phosphorus modified alloy heated to 735°C (1355°F), 785°C (1445°F), 850°C (1562°F) and solidified at an average cooling rate of approximately 1.3°C/s. The corresponding microstructures are presented in Figure 3. The numbered arrows correspond to the metallurgical reaction and are outlined in Table 2b.

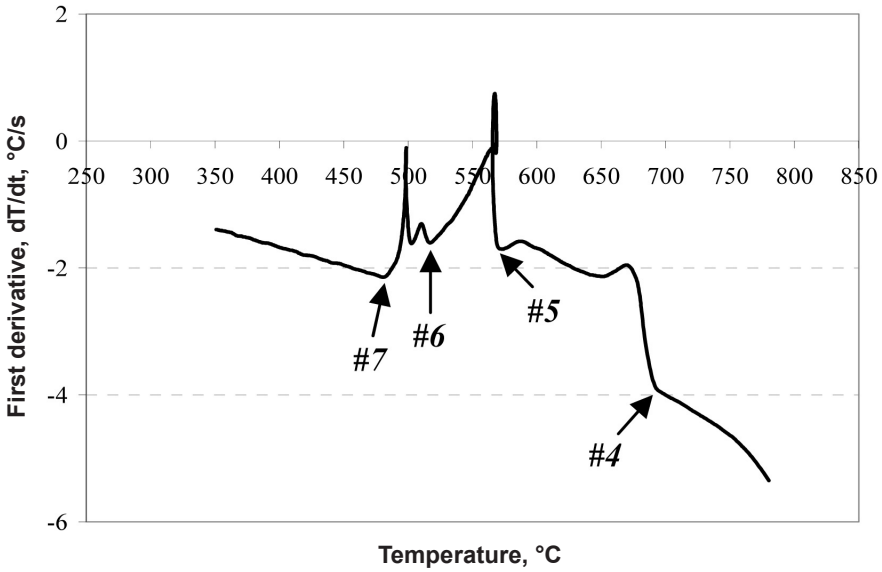

Figure 2b. First derivative vs. temperature cooling curve recorded during the solidification cycle of the Al-20%Si phosphorus modified alloy heated to 785°C (1445°F) and solidified at an average cooling rate of approximately 1.3°C/s.

Based on the analysis of the first derivative of the cooling curve (CR = 1.3°C/s) the liquidus temperature was determined at 685.5°C (1265.9°F) (Figure 2b). At this temperature the first primary Si crystals nucleated from the melt. Evolved latent heat caused the temperature of the surrounding melt to rise. This point was clearly visible as a sudden change occurred in the first derivative curve (point #4 in Figure 2b). As the solidification process continued to progress, the primary Si crystals continued to grow. At 566°C (1050.8°F) the next abrupt change in the first derivative curve corresponded with the nucleation of the Al-Si eutectic (point #5 in Figure 2b). The latent heat of the eutectic silicon is approximately 1800kJ/kg (as compared with 390kJ/kg for aluminum) and was sufficient to increase the melt temperature during

the solidification process.[8,32] This was manifested by the positive value of the first derivative peak (Figure 2b). This phenomenon relates to the so-called recalescence effect.[14,29,33] The depression of the Al-Si eutectic temperature can be related to the chemical and/or thermal modification of the Al-Si eutectic. The Si refinement level can be determined using both metallographic and thermal analysis techniques. A further decrease in the melt temperature resulted in the nucleation of the Cu based intermetallic phases at 512.9°C (955.2°F) (point #6 in Figure 2b). The convoluted peaks on the first derivative curve suggested that more than one spatially interrelated phase nucleated during the last stage of the solidification process. It was found that non-equilibrium liquidus was not affected by the melt temperature and was approximately 685°C (1265°F) for all analyzed test samples solidified at a cooling rate of 1.3°C/s. A similar observation was made for other metallurgical reactions, i.e., nucleation of the Al-Si eutectic, the Cu based phases and the solidus temperature.

Metallographic observations revealed the effect of the melt temperature on the size of the primary Si crystals for the alloy that solidified under an average cooling rate of 1.3°C/s (Figures 3 and 4). The ED of the primary Si particles was 96.9±32.7µm for the melt heated to 735°C (1355°F) and 75.8±19.4µm and 79.2±23.9µm for 785°C (1445°F) and 850°C (1562°F) respectively. The low melt heating temperature (i.e. 735°C/1355°F) resulted in coarse primary Si crystals and their heterogeneous distribution. It was found that the melt heated to 850°C (1562°F) had a slightly coarser average ED of primary Si particles than the melt heated to 785°C (1445°F). However, the 3.4µm difference between the ED was not statistically significant which also indicated the overlapping standard deviation for these test samples. Image analysis showed that the SDAS was between 31.9 and 34.4µm (Figure 5) for the test samples heated to 735°C (1355°F), 785°C (1445°F) and 850°C (1562°F) and these differences were not statistically significant.

a) 735°C/1355°F (ED = 96.9µm±32.7).

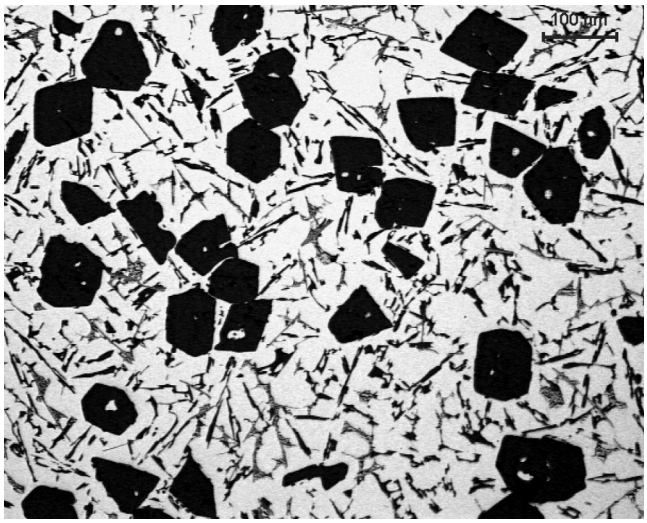

b) 785°C/1445°F (ED = 75.8µm±19.4).

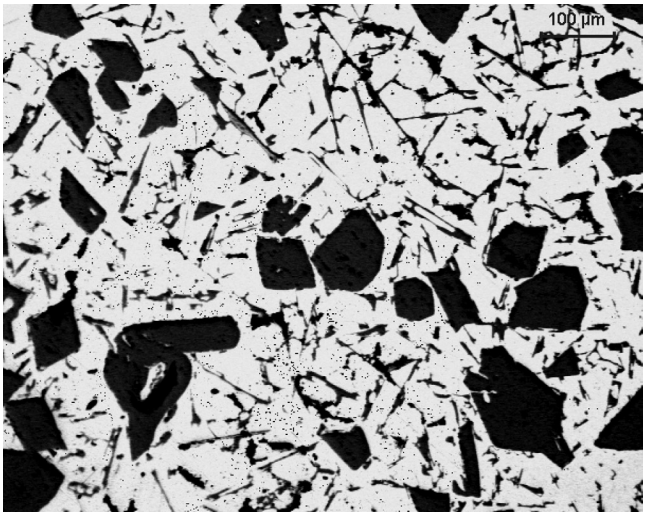

c) 850°C/1562°F (ED = 79.2µm±23.9).

Figure 3. Optical micrographs (100x) of the Al-20%Si phosphorus modified alloy test samples with the corresponding ED of the primary Si solidified at an average cooling rate of approximately 1.3°C/s. The alloy was heated to the ftemperatures as noted.

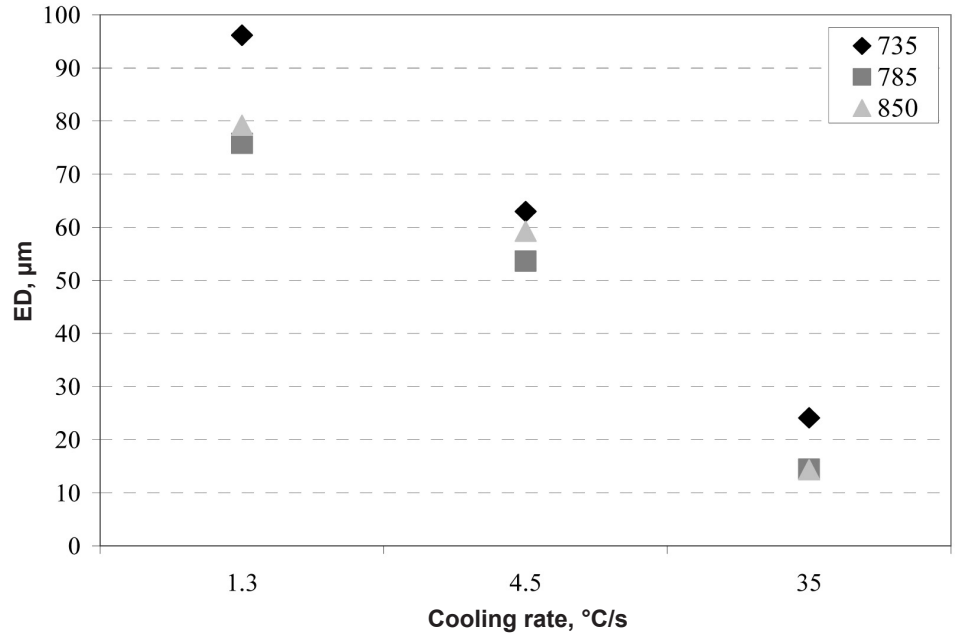

Figure 4. The equivalent diameter (ED) of the primary Si for the Al-20%Si phosphorus modified alloy heated to 735°C (1355°F), 785°C (1455°F), 850°C (1562°F) and solidified at an average cooling rate of approximately 1.3, 4.5 and 35°C/s.

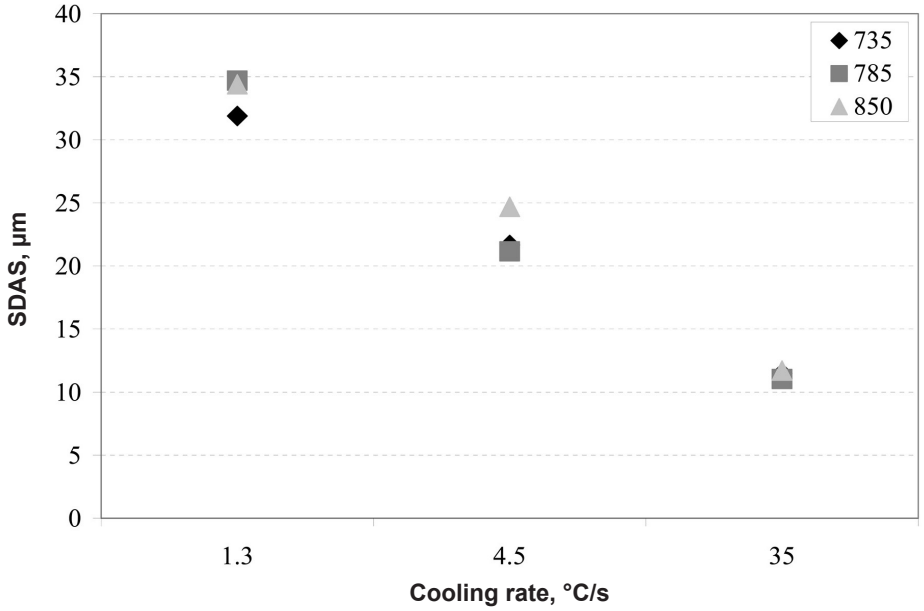

Figure 5. The secondary dendrite arm spacing (SDAS) of α-aluminum for the Al-20%Si phosphorus modified alloy heated to 735°C (1355°F), 785°C (1455°F), 850°C (1562°F) and solidified at an average cooling rate of approximately 1.3, 4.5 and 35°C/s.

Temperature vs. time cooling curves for the test samples heated to 735°C (1355°F), 785°C (1445°F) and 850°C (1562°F) and solidified at an average cooling rate of 4.5°C/s are presented in Figure 6a. The maximum instantaneous cooling rate was approximately 13°C/s as determined at the non-equilibrium liquidus temperature (Figure 6b). Spatial resolution of the cooling curves remained satisfactory despite the considerable increase in the cooling rate. Three (3) temperature arrests were visible on the temperature vs. time cooling curves (Figure 6a). The representative first derivative vs. temperature curve recorded for the test sample heated to 785°C (1445°F) and solidified at an average

cooling rate of 4.5°C/s is presented in Figure 6b. The metallurgical reactions are pointed out by the numbers and the corresponding numerical values are presented in Table 2b. The non-equilibrium liquidus temperature remained unchanged for the analyzed melt temperatures and was found to be 700.9°C (1293.6°F) (point #4 in Figure 6b). This value was approximately 15°C (59°F) (higher than for the test samples heated to identical temperatures but solidified at a slower average cooling rate, i.e., 1.3°C/s. This indicated that the non-equilibrium liquidus temperature was a function of the cooling rate only for these particular experimental conditions i.e. chemical refinement.

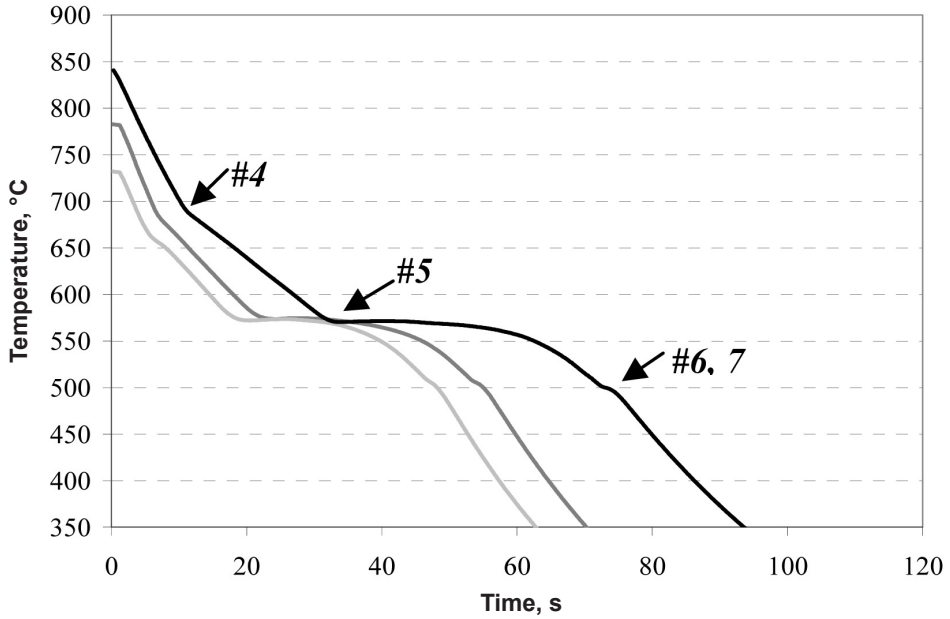

Figure 6a. Temperature vs. time cooling curves recorded for the Al-20%Si phosphorus modified alloy heated to 735°C (1355°F), 785°C (1455°F), 850°C (1562°F) and solidified at an average cooling rate of approximately 4.5°C/s. Arrows correspond to the metallurgical reactions recorded during the solidification process. Detailed values are presented in Table 2b. The corresponding microstructures are presented in Figure 7.

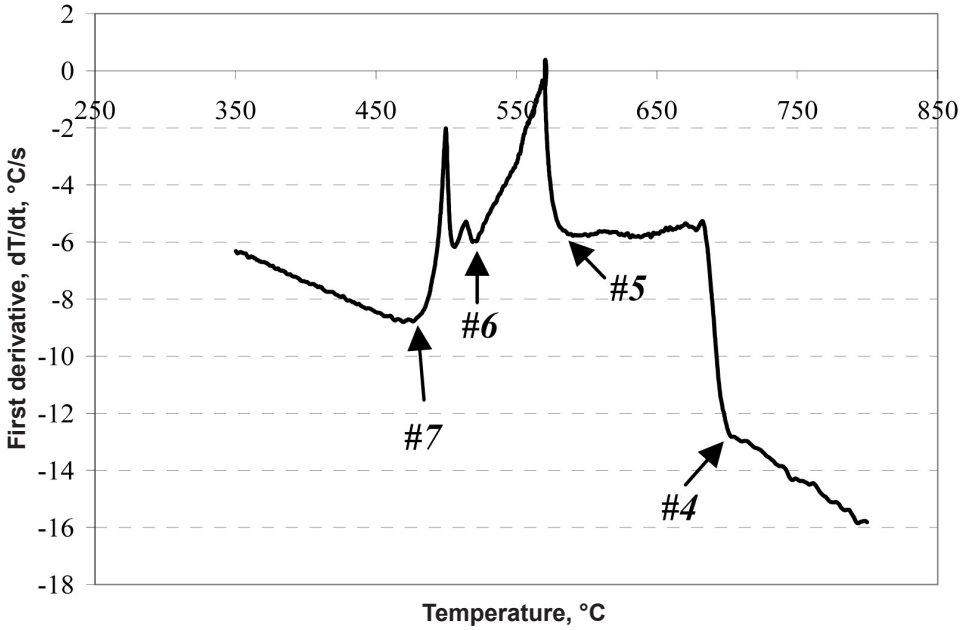

Figure 6b. First derivative vs. temperature cooling curve recorded during the solidification cycle of the Al-20%Si phosphorus modified alloy heated to 785°C (1455°F) and solidified at a cooling rate of approximately 4.5°C/s.

Metallographic observations of the test samples that solidified under an average cooling rate of 4.5°C/s revealed coarser primary Si for the melt heated to 735°C (1355°F) compared with 785°C (1445°F) and 850°C (1562°F) (Figure 7). The ED of the primary Si particles was found to be 62.9±20.3µm (for 735°C/1355°F), 53.6±12.7 (for 785°C/1445°F) and 59.2±12.1µm (for 850°C/1562°F). It was observed that the microstructure of the test sample heated to 735°C (1355°F) was less homogenous as far as the primary Si particle distribution was concerned. This phenomenon was clearly manifested by the approximate double standard deviation as compared with the test samples heated to 785°C (1445°) and 850°C (1562°F). The test sample heated to 850°C (1562°F) had a slightly larger ED of primary Si particles than the samples heated to 785°C (1445°F), but this difference was not statistically significant.

It was observed that the test samples solidified at an average cooling rate of 4.5°C/s had an SDAS in the range of 21.7 - 24.7µm (Figure 5) for the melt heated to the temperature range of 735°C (1355°F) to 850°C (1562°F). The difference in the average SDAS between the analyzed test samples was not statistically significant. These observations were in agreement with the image analysis performed for the test samples solidified at an average cooling rate of 1.3°C/s except for the value of the SDAS that was approximately 30% smaller for the test samples solidified at an average cooling rate of 4.5°C/s.

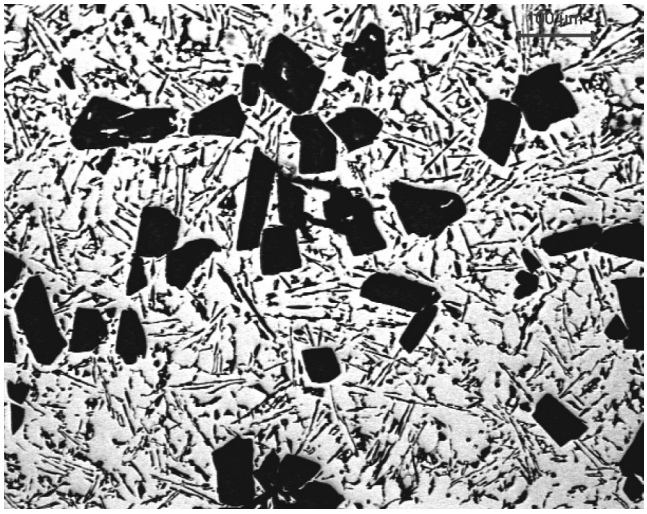

a) 735°C/1355°F (ED = 62.9µm±20.3).

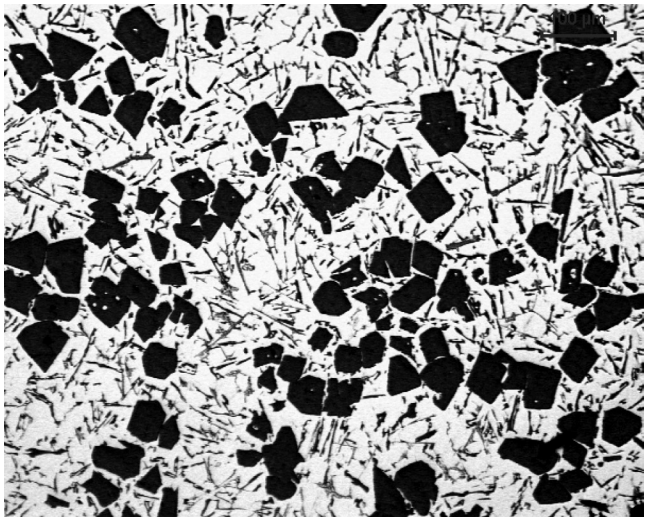

b) 785°C/1455°F (ED = 53.6µm±12.7).

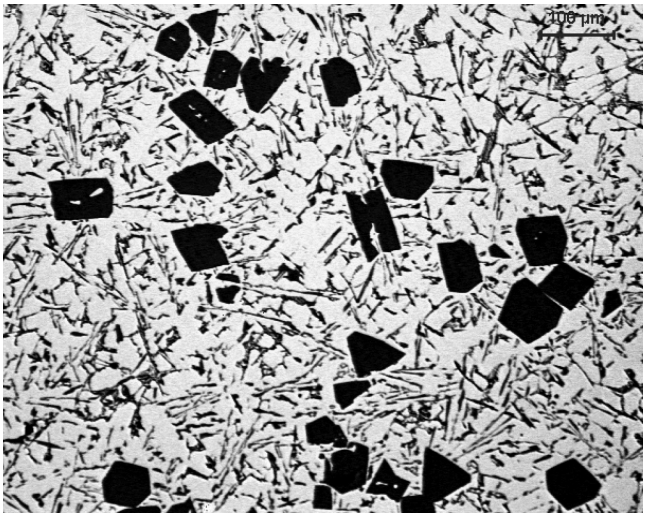

c) 850°C/1562°F (ED = 59.2µm±12.1).

Figure 7. Optical micrographs (100x) of the Al-20%Si phosphorus modified alloy with the corresponding ED of the primary Si solidified at an average cooling rate of approximately 4.5°C/s. The alloy was heated to the temperatures as noted.

Rapid Solidification Experiments Using a Copper Mold

Metallurgical data generated from the rapid solidification experiments showed a vital phenomenon that allowed for control of the size of the primary Si particles as a function of the melt temperature. It was observed that the test sample heated to 735°C (1355°F) and rapidly solidified inside a water cooled copper mold had an average ED of the primary Si particle equal to 24.1±7.1µm (Figure 8a). This value was approximately 40% higher in comparison with the test samples heated to 850°C (1562°F) (ED=14.3±2.9µm) and solidified under identical conditions (Figure 8b). Microstructure observations and calculated standard deviations (7.1 vs. 2.9µm for the lower and higher melt temperatures) for the average ED revealed that the distribution of the primary Si particles was associated with their size. Fine primary Si particles were significantly more homogeneously distributed in the aluminum matrix.

Image analysis of the test samples heated to 735°C (1355°F) and 850°C (1562°F) revealed that the SDAS remained unchanged and was approximately 11µm (Figure 5). Consistent values for the SDAS indicated good thermal management of the copper mold and satisfactory repeatability of the experimental parameters.

Discussion

Accurate thermal characteristics including fraction solid and liquid during melting and solidification cycles are of paramount importance for optimization of various metal casting technologies. However, this data is not readily available especially for the non-equilibrium industrial processing conditions. For example, fraction liquid vs. temperature data is necessary for determination of the ingot's heating temperature ensuring robust and economical semi-solid casting technologies rendering high quality components.[34] Conventional laboratory quenching experiments from pre-determined temperatures (between the liquidus and solidus) combined with quantitative metallographic analysis commonly used for the determination of fraction liquid often render biased results. Current studies demonstrated the ability to quantify various thermal characteristics of the multi-component alloys that are processed under industrially relevant conditions. For example, generated data for the Al-20%Si alloy indicated that at 585°C (1085°F) the volume of primary Si crystals was approximately 17% and this solid phase was suspended in 83% of the liquid melt. Melting of the primary Si crystals was completed at approximately 702°C (1295.6°F) when the melt reached the liquidus temperature.[6,7]

Characteristic temperatures of the metallurgical reactions obtained during Al-20%Si alloy solidification from 785°C (1445°F) at 1.3°C/s cooling rate are presented in Figure 2 and are summarized in Table 2b. This data indicates that the melt temperature did not affect the sequence of the metallurgical reactions. The non-equilibrium liquidus, nucleation of the Al-Si eutectic, nucleation of the Cu based phases and the solidus temperatures stayed within the ±3°C range during solidification cycles from 735°C (1355°F), 785°C (1445°F) and 850°C (1562°F). This low scatter was commonly observed during thermal analysis experiments and was most likely caused by sample heterogeneity.

Figures 2, 6, 10 and Table 2b indicate that during the non-equilibrium solidification process the liquidus temperature was increased by approximately 28°C (82.4°F) when the average cooling rate was increased from 1.3 to

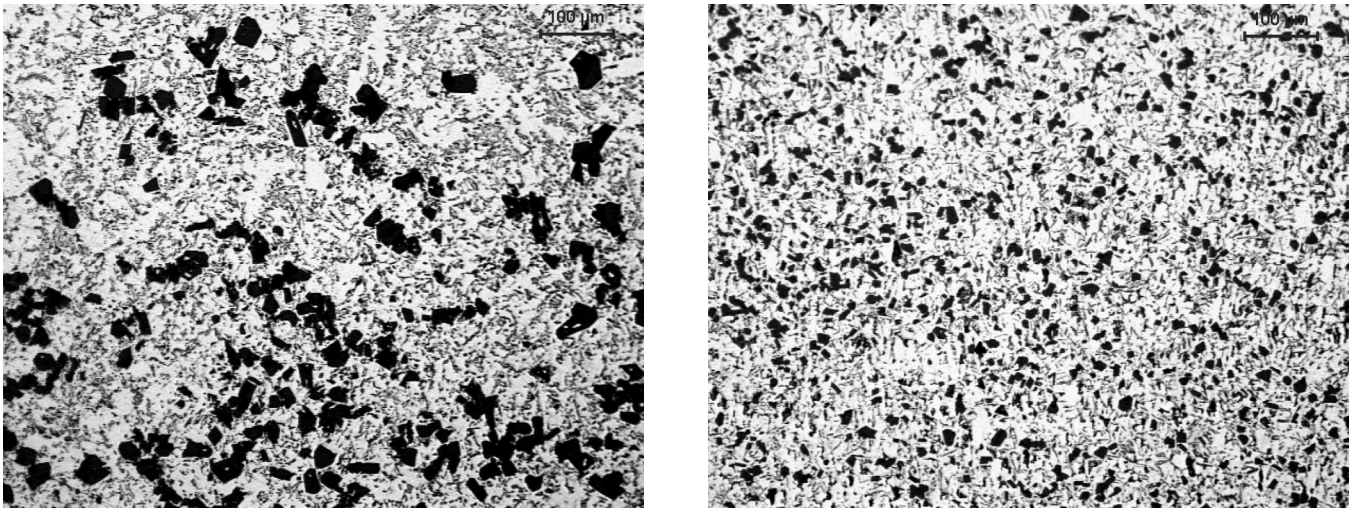

a) 735°C/1355°F (ED = 24.1±7.1µm). *b) 850°C/1562°F (ED = 14.3±2.9µm).*

Figure 8. Optical micrographs (100x) of the Al-20%Si phosphorus modified alloy with the corresponding ED of the primary Si heated to the following temperatures and solidified at an average cooling rate of approximately 35°C/s inside the water cooled copper mold as noted.

15°C/s (instantaneous from 4 to 35°C/s). The solidus temperature shifted up by approximately 5°C (41°F) from 477°C (890.6°F) to 482°C (899.6°F) while the average cooling rate increased from 1.3 to 15°C/s. Accordingly, the solidification range increased from approximately 208°C (406.4°F) to 231°C (447.8°F). Most likely the cause of the liquidus and solidus temperature shift might be the thermal signal drag caused by the temperature gradient inside the test samples that developed during the solidification process. Moreover, the observed shift of the liquidus temperature might be affected by the elevated concentration of Si in the liquid prior to its nucleation temperature. This could be a localized phenomenon characteristic of an undercooled melt where the diffusion process was restricted. The origin of this occurrence pertained to the fact that chemical changes dictated by the equilibrium phase diagram were unable to respond to the rapid temperature change forced by the heat flow. Consequently, the alloy solidification path had changed and the phase diagram was no longer obeyed. This resulted in the generation of chemical heterogeneous spots on the micro scale. Observed phenomenon might indicate that the liquid metal thermal characteristics were different than those obtained from the simple phase diagram. In turn, a change in nucleation temperatures for certain metallurgical reactions might affect the alloy's microstructure and consequently its service characteristics.[8,33] The detailed contribution and its overall effect have to be further validated and determined. Thermal analysis experiments under different cooling rates performed for steels with various carbon levels showed a similar trend for the liquidus temperature increase. The scientific explanation of this phenomenon was not presented.[35]

It was found that the test sample heated to 735°C (1355°F) had the coarsest primary Si crystals that were heterogeneously distributed within the metal matrix. The ED of primary Si crystals was reduced and homogeneity improved when the melt was heated to 785°C (1445°F) and 850°C (1562°F). This most likely indicated that the melt had a heterogeneous distribution of Si clusters having a short range atomic order. Most of these heterogeneities acted as solidification sites and facilitated the primary Si nucleation.[36] They existed in the liquid despite the fact that liquidus temperature was exceeded by approximately 33°C (91.4°F). Analysis of the binary Al-P diagram provided additional explanation indicating that higher melt temperature increased the amount of phosphorus dissolved in the melt leading to more Al-P nucleation sites. Consequently, the primary Si crystals grew around the Al-P nuclei at the rate controlled by the diffusion of the Si atoms in the liquid melt. It was observed that the as-cast microstructure homogeneity was considerably improved by increasing the melt temperature from 735°C (1355°F) to 785°C (1445°F) and to 850°C (1562°F). It is worth noting that melt heating to 850°C (1562°F) resulted in coarser primary Si crystals than the melt heated to 785°C (1445°F) however, this difference was not statistically significant. However, for some metallurgical applications even such a small difference of primary Si size could be beneficial. Therefore, this data indicated that the melt temperature near 785°C (1445°F) for the low cooling rates and the level of phosphorus addition utilized in these experiments could be optimal. Similar observations were reported by Telang[37] for the Al-21%Si alloy modified with 0.2% phosphorus. It was found that melt heating above approximately 900°C (1652°F) resulted in coarsening of the primary Si for the test sample solidified inside the water cooled steel crucible. It was suggested that the Al-P particles started to disintegrate or even melt above 900°C (1652°F) and caused a coarsening effect of primary Si crystals. Most likely a higher melt temperature was more efficient in minimizing the effect of the preferred atomic Si arrangement and the liquid melt was capable of losing some of the heterogeneities. Conclusions from the current studies have practical applications indicating that for the targeted level of phosphorus addition, i.e. 100ppm, the size of the primary Si crystals was a function of the melt temperature for a given cooling rate. It has to be stressed out that potency for Si crystal chemical refinement could vary due to the differences in the amount of phosphorus dissolved in the melt at the specific temperature. To gain the full benefits of thermal refinement the melt temperature has to be properly optimized and controlled.

In-situ temperature measurements carried out by the authors during the HPDC industrial trials indicated that the Al-20%Si melt at 785°C (1455°F) poured into the dossing hole had a temperature in the range 730°C (1346°F) to 680°C (1256°F) (centre vs. wall location). Such low melt temperature caused pre-mature nucleation of the primary Si crystals before entering the die cavity. Consequently, this reduced the effectiveness of primary Si refinement and overall casting homogeneity.[6] Complex melt temperature profile, as observable during the LPPM or HPDC processing, was difficult to replicate during the laboratory experiments. The controlled solidification experiments, as presented in this publication, were crucial to understanding the behaviour of the hypereutectic alloy under various casting processing parameters. Results from these studies were implemented to optimize the permanent mold casting process.

Image analysis data indicated that for the slow cooling rate, the SDAS was not affected by the melt temperature (from 735°C/1355°F to 850°C/1562°F). The average SDAS was 33.7±1.5μm for a 1.3°C/s and 22.5±0.9μm for a 4.5°C/s cooling rates (Figure 5). Please note the very small SDAS standard deviation. These experiments confirmed that the high cooling rates reduced the time necessary for coarsening of the α-aluminum dendrites. This phenomenon resulted in multiplication of the secondary dendrite arms that distributed the solute content in front of the solidifying interface. It was also observed that the

pockets of α-aluminum dendrites were less distinguishable from the non-dendritic metal matrix for a low cooling rate as compared with the test samples that solidified under a high cooling rate.[38]

Rapid solidification experiments in the copper mold were carried out to validate the experiments performed using a relatively slow cooling rate and to evaluate the alloy's response to the thermal conditions that are equivalent to the permanent mold casting. The results from these experiments confirmed previous findings obtained for 1.3 and 4.5°C/s cooling rates. It was observed that the size of the primary Si crystals in the test samples solidified inside the copper mold was reduced by approximately 40% (from 24.1±7.1 to 14.3±2.9μm) as a result of intensified thermal refinement when the melt temperature was increased from 735°C (1355°F) to 850°C (1562°F) (Figures 4 and 8). Rapid cooling (in comparison with Figures 3 and 7) resulted in a higher number of nucleation sites for the primary Si crystals and restricted their growth by reducing the time necessary for the diffusion process. Consequently, the size of the primary Si crystals was reduced with a significant increase in the cooling rate.[6,7,38] It was also observed that higher cooling rates minimized the variation of primary Si crystal size that was expressed by the smaller standard deviation.

Experimental results indicated that the melt heated to 850°C (1562°F), homogenized and slowly cooled in the holding crucible from 850°C (1562°F) to 730°C (1346°F) prior to casting into the copper mold exhibited relatively coarse primary Si crystals and a fine Al-Si eutectic structure (Figure 9). This experiment resulted in the primary Si crystals ED being 27.2±8.2μm and the SDAS being 10.1±2.2μm. The effect of the melt's high temperature was lost as far as the thermal refinement of the primary Si crystals was concerned despite the high solidification rate achieved in the copper mold. The overall primary Si refinement was almost identical to the melt heated to 735°C (1355°F) and cast under identical conditions (Figures 8a and 9). These results indicated that slow cooling of the melt in the holding crucible from 850°C (1562°F) to 730°C (1346°F) prior to the casting operation most likely resulted in the formation of a preferred arrangement of Si atoms in the liquid that in turn resulted in coarser primary Si crystals. Please note that in this experiment the pouring was done at approximately 45°C (113°F) above the liquidus temperature. A similar situation can be observed in permanent mold castings where the melt loses its temperature during prolonged transferring and pouring as well as flowing through the gating system before the filling of the mold cavity. Therefore, when the melt temperature and handling are not optimized, than the melt entering the die cavity is at a temperature too close to the liquidus. Consequently, the primary Si crystals are coarser and heterogeneously distributed. These experiments showed the importance of melt temperature control prior to entering the mold. The Al-20%Si melt processing conditions were representative of the industrial environment (except 850°C/1562°F) and were chosen to underline the sensitivity of primary Si size to melt as well as pouring temperatures. Melt temperature of 850°C (1562°F) would not be acceptable in the production environment due to its negative effect on productivity and tool life. This would also result in excessive melt oxidation and elevated hydrogen levels. Typical casting temperatures for HPDC, LPPM and Sand Casting are between 680-700°C (1256-1292°F), 730-780°C (1346-1436°F) and 725-760°C (1337-1400°F) respectively.

Figure 10 presents high resolution temperature vs. time (a) and first derivative vs. temperature (b) curves recorded at a 2000Hz acquisition rate during rapid solidification experiments with an average cooling rate of 15°C/s. The compressed helium gas at 10MPa pressure was used as a quenching medium. The first derivative cooling curve showed highly similar thermal events in comparison with the derivative curves obtained at an average cooling rates of 1.3°C/s (Figure 2b) and 4.5°C/s (Figure 6b).

The controlled solidification experiments allowed for the production of metallographic samples for image analysis and the related thermal characteristics for statistical analysis of their relationship. Comparative image analysis of the cast component with the laboratory generated structures allowed for the determination of the solidification characteristics of the component's given section.[6]

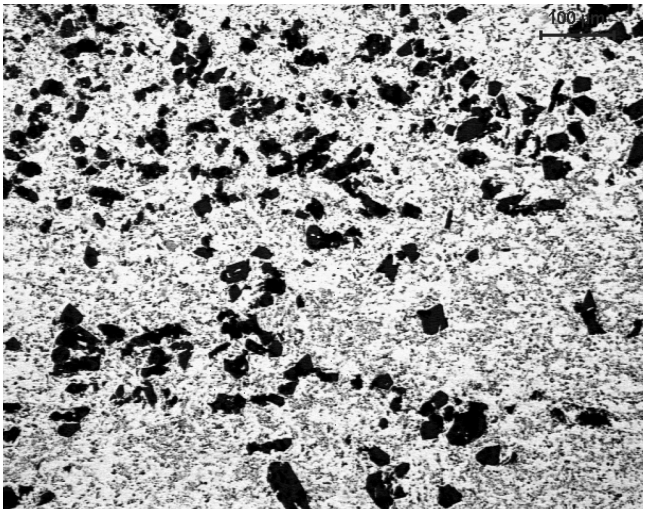

Figure 9. Optical micrographs (100x) of the Al-20%Si phosphorus modified alloy heated to 850°C (1562F) and cast from 730°C (1346F) into the water cooled copper mold at a cooling rate of approximately 35°C/s. The ED of the primary Si was 27.2±8.2μm and the SDAS was 10.1±2.2μm.

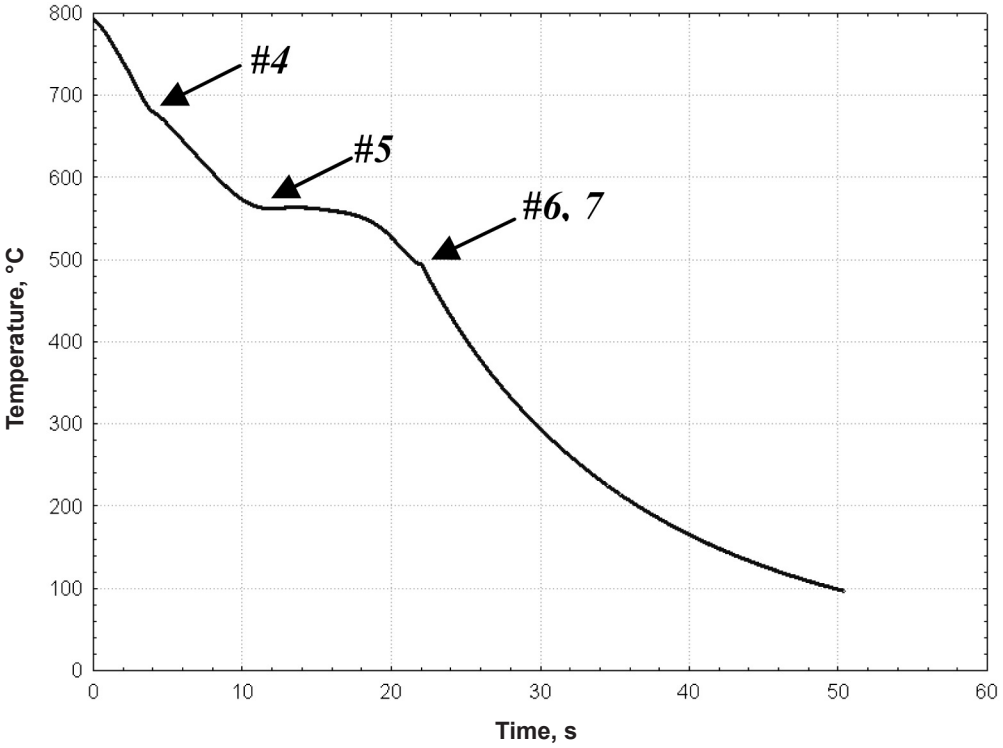

Figure 10a. Temperature vs. time cooling curve recorded during the solidification cycle of the Al-20%Si phosphorus modified alloy heated to 785°C (1455°F) and solidified under forced helium gas at an average cooling rate of approximately 15°C/s. Numbered arrows correspond to the metallurgical reactions recorded during the solidification process. Detailed values are presented in Table 2b.

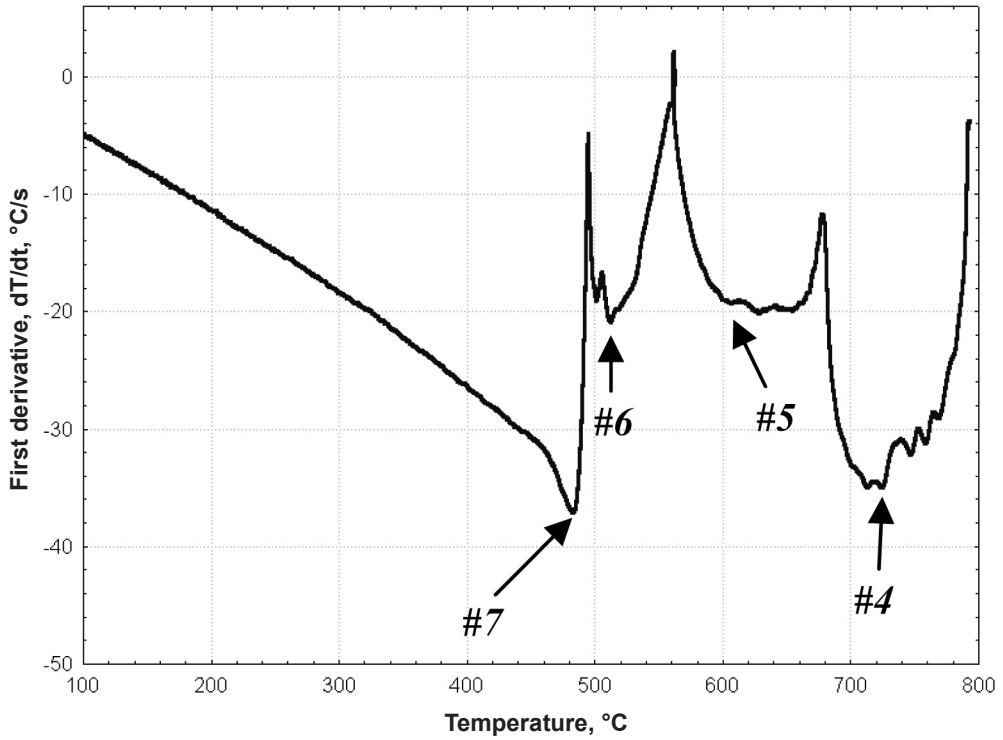

Figure 10b. First derivative vs. temperature cooling curve recorded during the solidification cycle of the Al-20%Si phosphorus modified alloy heated to 785°C (1455°F) and solidified under forced helium gas at an average cooling rate of approximately 15°C/s.

Conclusions

The conclusions pertaining to the effects of the melt temperature as well as the solidification rate on the structural and thermal characteristics of the Al-20%Si high pressure die casting alloy are as follows:

a) Higher melt temperatures (785°C/1445°F and 850°C/1562°F) had a positive effect on the size and distribution of the primary Si crystals while excessive melt temperature might not be acceptable in the production environment. Melt heated to 735°C (1355°F) resulted in coarse and heterogeneous primary Si crystals. This phenomenon was observed for all analyzed cooling rates, i.e., 1.3, 4.5, 15 and 35°C/s.

b) A significant increase in the cooling rate during the solidification process minimized the variation of the primary Si crystal size and heterogeneity caused by the melt temperature.

c) Melt pouring close to the liquidus temperatures (i.e., 730°C/1346°F) resulted in coarse primary Si crystals despite the melt's high initial temperature i.e., 850°C (1562°F).

d) The SDAS was not affected by the melt temperature and was a function of the cooling rate for all experimental conditions. The SDAS decreased from approximately 32 to 22µm for a 1.3 and 4.5°C/s cooling rate and was further reduced to approximately 11µm for the copper mold experiments where the cooling rate was estimated as 35°C/s.

e) The likely reason for the primary Si crystal size dependence on the melt temperature could be the presence of heterogeneous clusters of short range Si atoms that existed above the liquidus temperature.

f) The melt heated to 735°C (1355°F), 785°C (1445°F), 850°C (1562°F) did not have an effect on the sequence of the metallurgical reactions during the alloy solidification process at an average cooling rate of 1.3, 4.5 and 15°C/s, except that the nucleation of the primary Si and the Al-Si eutectic was shifted toward higher values with an increase in the cooling rate.

g) Cooling curves and their derivatives for average cooling rates of 1.3, 4.5 and 15°C/s had a satisfactory spatial resolution which in turn allowed for the determination of the thermal characteristics and the correlation with the test sample microstructures. This data represents a valuable input for the computer modeling of non-equilibrium solidification conditions.

Acknowledgements

The authors would like to thank Mr. John Jorstad from JLJ Technologies Inc. (USA) for his valuable comments to this manuscript, Mrs. Marta Aniolek from CANMET-MTL (Canada) for data analysis as well as Mr. Marcin Kasprzak from the Silesian University of Technology (Poland) for his contributions to the solidification experiments. Moreover, the authors would also like to acknowledge the long term support for the University of Windsor's Light Metals Casting Technology Group by AUTO21, a member of the Networks of Centres of Excellence of Canada.

REFERENCES

1. Ghosh S., Mott W.J., "Some Aspects of Refinement of Hypereutectic Al-Si Alloys", AFS Transactions, vol. 72, pp 721-732 (1964).
2. Henslar P., "The New Porsche 944 4-Cylinder Aluminum Engine", SAE Paper No. 830004 (1983).
3. Jorstad J.L., "Reynolds 390 Engine Technology" SAE Paper No. 830010 (1983).
4. Legge R. A., Smith D. M., Henkel G., "Improved Aluminium Alloy for Engine Applications", SAE Paper No. 860558 (1986).
5. Reuss L.E., Hughes C. N., SAE Paper No. 710150 (1971).
6. Yamagata H., Kasprzak W., Aniolek M., Kurita H., Sokolowski J.H., "The Effect of Average Cooling Rates on the Microstructure of the Al-20% Si High Pressure Die Casting Alloy used for Monolithic Cylinder Blocks", Journal of Materials Processing Technology, vol. 203, pp 333-341 (2008).
7. Yamagata H., Kurita H., Aniolek M., Kasprzak W., Sokolowski J.H., "Thermal and Metallographic Characteristics of the Al–20% Si High-Pressure Die-Casting Alloy for Monolithic Cylinder Blocks", Journal of Materials Processing Technology, vol. 199, no. 1-3, pp 84-90 (2008).
8. Tenekedjiev N., Gruzleski J.E., "Hypereutectic Aluminum-Silicon Casting Alloys – A Review", Cast Metals, vol. 3, no. 2, pp 96-105 (1990).
9. Yamagata H., "The Science and Technology of Materials in Automotive Engines", Woodhead Publishing, Cambridge, (2005).
10. Kamble S., Ravindran C., "Analysis of Primary Silicon Crystals in Hypereutectic Aluminum-Silicon Alloys: Effect of Change in Process Parameters", AFS Transactions, vol. 113, pp 87-97 (2005).
11. Kim M., "Electron Back Scattering Diffraction (EBSD) Analysis of Hypereutectic Al-Si Alloys Modified by Sr and Sc", Metals and Materials International, vol. 13, no. 2, pp 103-107 (2007).

12. Li J., Elmadagli M., Gertsman V.Y., Lo J., Alpas A.T., "FIB and TEM Characterization of Subsurfaces of an Al-Si Alloy (A390) Subjected to Sliding Wear", Materials Science and Engineering A, vol. 421, no.1-2, pp 317-327 (2006).
13. Xu C.L., Yang Y.F., Wang H.Y., Jiang Q.C., "Effects of Modification and Heat Treatment on the Abrasive Wear Behavior of Hypereutectic Al-Si Alloys", Journal of Materials Science, vol. 42, no. 15, pp 6331-6338 (2007).
14. Djurdjevic M. B., Kasprzak W., Kierkus C.A., Kierkus W.T., Sokolowski J.H., "Quantification of Cu Enriched Phases in Synthetic 3XX Aluminum Alloys using the Thermal Analysis Technique", AFS Transactions, vol. 16, pp 1-12 (2001).
15. Yamagata, H., Kurita, H., "Effect of Elastic Deformation of the Honing Stone on the Exposure of Si-Crystals in a Hyper-Eutectic-Si Aluminum Cylinder Block", Society of Automotive Engineers of Japan. SAE Paper No. 20056577 (2005).
16. Donaule R.J., Hesterberg W.G., Cleary T.M., "Hypereutectic Aluminum-Silicon Alloy Having Refined Primary Silicon and a Modified Eutectic", U.S. Patent No. 5234514 (Aug. 1992).
17. Eady J.A., Smith D.M., "Properties and Applications of New Aluminum Foundry Alloy", SAE Paper No. 840123 (1984).
18. Shamsuzzoha M., Juretzko F.R., "Dual Refinement of Primary and Eutectic Silicon in Hyper-Eutectic Al-Si Alloys", Aluminum Alloys for Transportation, Packaging, Aerospace and Other Applications, pp 153-162 (2007).
19. Wang R-Y., Lu W-H., Ma Z-Y., "Electrolytic Hypereutectic Alloy Casting with Completely Eutectic Structure", AFS Transactions, vol. 115, pp 241-248 (2007).
20. Xiufang B., Weimin W., "Thermal-Rate Treatment and Structure Transformation of Al-13 wt% Si Alloy Melt", Materials Letters, (44) 1 54-58 (2000).
21. Sigworth G. K., "Refinement of Hypereutectic Al-Si Alloys", AFS Transactions, vol. 95, pp 303-314 (1987).
22. Wang H., Ning Z.Z., Davidson C.J., St John D.H., Xie S.S., "Thixotropic Structure Formation in A390 Hypereutectic Al-Si Alloy", Proceedings of the 8th International Conference of Semi-Solid Processing, Limassol, Cyprus, Worcester Polytechnic Institute (2004).
23. Kasprzak M., Kasprzak W., Sokolowski J. H., U. S. Patent No. 7,255,828 (Aug. 14, 2007).
24. Dehong L., Yehua J., Guisheng G., Rongfeng Z., Zhenhua L., Rong Z., "Refinement of Primary Si in Hypereutectic Al-Si Alloy by Electromagnetic Stirring", Journal of Materials Processing Technology, vol. 189 (1-3) pp 13-18 (2007).
25. Takagi H., Uetani Y., Dohi M., Yamashita T., Matsuda K., Ikeno S., "Effects of Mechanical Stirring and Vibration on the Microstructure of Hypereutectic Al-Si-Cu-Mg Alloy Billets", Materials Transactions, vol. 48, no. 5, pp 960-966 (2007).
26. Youn J. IL., Kang B. II, Kim Y. J., "Ultrasonic Injection for Melts Modification of Hyper-eutectic Aluminum Alloy", Asian Forum of Light Metals & Exhibition. Kaohsiung, Taiwan (2007).
27. Kurita H., Yamagata H., "Hypereutectic Al-20%Si Alloy Engine Block using High-Pressure Die-Casting", Proceedings of the SAE 2004 World Congress & Exhibition, Detroit, USA, 2004-01-1028 (2004).
28. Chen X., Kasprzak W., Sokolowski J. H., "Reduction of the Heat Treatment Process for Al-based Alloys by Utilization of Heat from the Solidification Process", Journal of Materials Processing Technology, vol. 176, no.1-3, pp 24-31 (2006).
29. Kasprzak M., Kasprzak W., Kierkus C.A, Kierkus W.T., Sokolowski J.H., Evans W. J., "Structure and Matrix Microhardness of the 319 Aluminum Alloy After Isothermal Holding During the Solidification Process", AFS Transactions, vol. 16, pp 1-11 (2001).
30. Sokolowski J.H., Kierkus W.T., Kasprzak M., Kasprzak W., U.S. Patent No. 7,354,491 (April 8, 2008).
31. Onda H., Sakurai K., Masuta T., Oikawa K., Anzai K., Kasprzak W., Sokolowski J. H., "The Effect of Solidification Models on the Prediction Results of the Temperature Change of the Aluminum Cylinder Head Estimated by FDM Solidification Analysis", Trans Tech Publications, Switzerland, Materials Science Forum, 561-565 1967-1970 (2007).
32. Jorstad J.L., Apelian D., "Hypereutectic Al-Si Alloys: Practical Processing Techniques", Die Casting Engineer, vol. 48, no. 3, pp 50, 52, 54-56, 58 (2004).
33. Backerüd L., Chai G., Tamminen J., "Solidification Characteristics of Aluminum Alloys, Vol. 2. Foundry Alloys", American Foundry Society Inc., Stockholm, (1990).
34. Jorstad J.L., Apelian D., "Pressure Assisted Processes for High Integrity Aluminum Castings", International Journal of Metalcasting, vol. 2, no. 1, pp 19-39 (2008).
35. Jernkontoret Stockholm, "A Guide to the Solidification of Steels", pp 162, ISBN 91-7260-156-6 (1977).
36. Eskin G.I., Eskin D.G., "Some Control Mechanism of Spatial Solidification in Light Alloys", Zeitschrift fur Metallkunde, vol. 95, no. 8 (2004).
37. Telang Y.P., "Process Variables in Al-21Si Alloys Refinement", AFS Transactions, vol. 71, pp 232-240 (1963).
38. Weiss J.C., Loper Jr. C.R., "Primary Si in Hypereutectic Aluminum-Silicon Castings", AFS Transactions, vol. 95, pp 51-62 (1987).

The Effect of the Melt Temperature and the Cooling Rate On the Microstructure of the Al-20% Si Alloy Used for Monolithic Engine Blocks

W. Kasprzak and M. Sahoo, CANMET Materials Technology Laboratory, Ottawa, Ontario, Canada
J. Sokolowski, University of Windsor, Windsor, Ontario, Canada
H. Yamagata and H. Kurita, Yamaha Motor Co. Ltd., Iwata, Shizuoka, Japan

Reviewer: The ASM series on phase diagrams shows a constrained vapour phase diagram between Al and P showing the single congruently melting compound AlP. I draw the authors attention to the liquidus close to the aluminum side of this phase diagram. It comes down almost asymptotic to the Al axis i.e. the balance between the amount of P present in the melt as dissolved P and that present as AlP changes very rapidly as the temperature drops. Hold at higher temperatures before casting and the dissolved P content will be higher, with the likelihood of more and finer AlP particles precipitating out while the casting is actually solidifying. Hold at low temperatures and the opposite—much of the P maybe present as pre-existing larger AlP particles which have had time to form and grow while floating in the liquid before casting, perhaps even agglomerating and/or settling. This constitutes an alternative explanation for the tendency towards finer and better dispersed primary Si particles at higher melt temperatures.

Commercially, it is well known that hypereutectics, and indeed any alloys being P treated, need to be alloyed at higher temperatures in order to achieve the best recovery to the alloy of P from the master alloys. Melts held too cold simply never get beyond a set low concentration of P, as read by OES, no matter how much master alloy is added - most likely as limited by the P solubility limit. Raising the metal temperature and stirring will frequently result in an increased P reading in stubborn melts like this even without further AlP addition.

The statement that the P addition was identical (100ppm) in all samples is unlikely to be correct for the reasons outlined above. Its form is as important as its mere presence. It cannot be safely assumed that the P nucleating potential was the same for all samples for the reasons elaborated above. It would enhance the paper greatly for the authors to include this solubility argument as a possible explanation for the improvement in primary Si structure with temperature.

***Authors**: The suggestion made by the reviewer to incorporate into the manuscript the P solubility argument based on the Al-P phase diagram is greatly appreciated. This provided additional explanation about primary Si refinement as a function of melt temperature predominantly during the melting cycle. Primary Si refinement phenomenon gets more complex when properly preheated melt (i.e., with sufficient AlP nucleation sites) is sequentially cooled down at various rates during the casting process. Consequently, the primary Si grows around the AlP nuclei at the various rates controlled by the diffusion of the Si atoms in the liquid melt. The industrially relevant example and encountered difficulties pertaining to LPPM or HPDC processing are mentioned in this publication and they were frequently observed by other practitioners. It would be scientifically relevant to quantify the effect of the melt temperature profile, as observed in the industrial casting practice, on the primary Si refinement using thermal analysis technique. The variety of primary Si morphologies observed in unmodified and modified hypereutectic Al-Si alloys (hexagonal, star-shaped, dendritic, etc.) have been reported in the literature but unfortunately corresponding cooling curve parameters are not available. Such data would be crucial to define casting process parameters that would yield desired microstructure and provide an input for casting process control as well as solidification modeling software. Such research activities are being currently addressed by the authors.*

Reviewer: Table 1–0.01% P is a very loose analysis allowing for anything between 0.0095 and 0.0144 according to ASTM roundoff rules. A spectrometer properly set up to read this line should be capable of at least one more decimal point. It would also help the arguments that follow in the paper if the samples which underwent tests could be sparked to see if there is variation in P recovery with pouring temperature. P is not that stable an element in Al melts for the reasons elaborated in previous review comments.

***Authors:** Table 1 showing Al-20%Si alloy chemical analysis was amended by adding the range of P concentrations based on OES analysis. The P pre-modified ingots were used for all experiments. Additionally, to verify the alloy chemical composition the OES analysis was done for one melt processing conditions prior to the experiments. Authors agree that it would be beneficial to analyze each test sample after completion of the experiments to check the variation in P recovery with pouring temperature. This suggestion will be considered for future experiments. The 100ppm represented rather the target P concentration than actual instrument reading.*

Reviewer: The statement that the P addition was identical (100ppm) is at odds with the chemistry reported in Table 1 which does not list this many decimal points. Only one can be correct.

***Authors:** The final text has been amended for clarity: "...P addition was identical (100ppm) in all samples...". The target value of the P in this study was 100ppm and was typically used during industrial practice.*